UNIVERSITAT POLITÈCNICA DE CATALUNYA
BARCELONATECH
Escola d'Enginyeria de Barcelona Est

FINAL DEGREE PROJECT

Materials Engineering

ANALYSIS OF PMMA DISTRIBUTION AROUND SPINE CANNULATED PEDICLE SCREWS IN OSTEOPOROTIC LUMBAR AND SACRAL VERTEBRAE

Memory

Author: Gerard Cabestany Bastida
Director: Prof. Dr. Enrique Fernández Aguado
Codirector: Prof. Dr. Sergi Gómez González
Call: June 2017

Abstract

The main goal of this project has been to analyse the distribution of injected cement into vertebrae. The study has focused on the cement's behaviour around pedicle screws inserted into lumbar (L4 and L5) and sacral (S1) vertebrae of elder people who underwent vertebroplasty. Models of the screw and cement were obtained from Computed Tomography. Once treated with CAD software, the models were ready to be studied. Longitudinal and transversal views of the maximum injected cement profiles were obtained. From these profiles, results could be obtained. They showed a tendency of injected cement into S1 vertebra to behave asymmetrically compared to a more symmetrical and homogeneous behaviour shown when injected into L4 and L5 vertebrae. Thus, leading to the assumption that pedicle screws injected into L4 and L5 vertebrae have a better chance of success than those injected into S1 vertebra.

Acknowledgements

I would like to thank Dr. Enrique Fernández Aguado, Dr. Sergi Gómez González and Dr. Josep López López, Research Group of Interacting Surfaces in Bioengineering and Materials Science (InSup), Technical University of Catalonia (UPC) for their enormous help and support. And for showing me how a research team works and the difficulties one can find in real life when carrying out a project.

Also, I would like to thank Dr. Maria Daniela Vlad (Faculty of Medical Bioengineering, “Grigore T. Popa” University of Medicine and Pharmacy. Iasi, Romania) and Dr. Luis Álvarez Galovich (Hospital Universitario Fundación Jimenez Díaz, Spine Unit) for their contribution concerning clinical management of spine surgery procedures.

Summary

List of Figures

List of Tables

Preface

Background

This work is part of the project for which the InSup research team received public funding from MINISTERIO DE ECONOMIA, INDUSTRIA Y COMPETITIVIDAD.
Reference: DPI2016-77768-R
Beneficiary entity: UNIVERSITAT POLITECNICA DE CATALUNYA
Centre: ESCUELA TECNICA SUPERIOR DE INGENIERIA INDUSTRIAL DE BARCELONA
Main Researcher: ENRIQUE FERNANDEZ AGUADO
Execution time: From 20/12/2016 to 29/12/2019

Title: OBTENCIÓN, DISEÑO, CARACTERIZACIÓN, MODELIZACION E IMPRESION 3D, EN LA MACRO/MICROESCALA, DE TEJIDOS OSEOS Y DE ANDAMIOS BIOMIMETICOS PARA INGENIERIA DE TEJIDOS.

From November, date when I started working with the InSup research team, the objective of the project was to reveal the microstructural features of different vertebrae. Particularly, lumbar and sacral vertebrae. Permeability studies of different regions of these vertebrae were intended to be carried out in order to deepen our knowledge of its internal structure. Thus, helping improve currently used surgical techniques.

After several weeks of bibliography research and becoming familiar with the software used by the InSup group (ScanIP, SolidWorks, Rhinoceros, Invesalius), we received the Computed Tomography scans of the spine but with low quality. Thus, making any permeability calculation impossible. At that point, the project was lightly modified. There was data about injected cement distribution on vertebrae obtained from the above-mentioned project, which after being treated with CAD software, needed further analysis. So, my first task has been to analyse all the collected clinical data about the patients and then write a research article with the goal of getting it published at an international Journal.

Apart from this task, I have also worked in designing new scaffolds for bone tissue engineering with the help of CAD software, Rhinoceros. However, issues with the running time of CFD and mechanical simulation has prevented us from achieving any results for now. For confidentiality concerns and the lack of results (apart from the models themselves, with their characterization), it was decided not to include this part of the work to the Final Degree Project.

To sum up, my goal in joining Dr. Enrique Fernández Aguado and Dr. Sergi Gómez González has been to understand how a Research team works and help them in the projects they were – and still are – working on.

1. Introduction

1.1. Anatomy of the Spine

The spine is the central axis of the skeleton and here lies its importance. It is responsible for supporting the body, protecting the spinal cord and spinal nerve roots and allow the movement of the trunk. To fulfil these requirements, the spine consists of a series of bones (vertebrae) which give rigidity to it and soft tissues (intervertebral joints) which give flexibility to it.

It is composed of 33 vertebrae, divided into 4 parts: 7 vertebrae in the cervical region (C1-C8), 12 in the thoracic region (T1-T12), 5 in the lumbar region (L1-L5) and 9 that are fused in the sacrum and coccyx (Fig. 1.B). It develops 4 curves (as can be observed in Fig. 1.A); two lordosis (that are convex anteriorly) and two kyphoses (that are convex posteriorly). The primary curves are kyphoses (thoracic and pelvic) and appear at the earliest stages of fetal development. The secondary curves are the lordosis (cervical and lumbar) and are often not detected until the postnatal period.

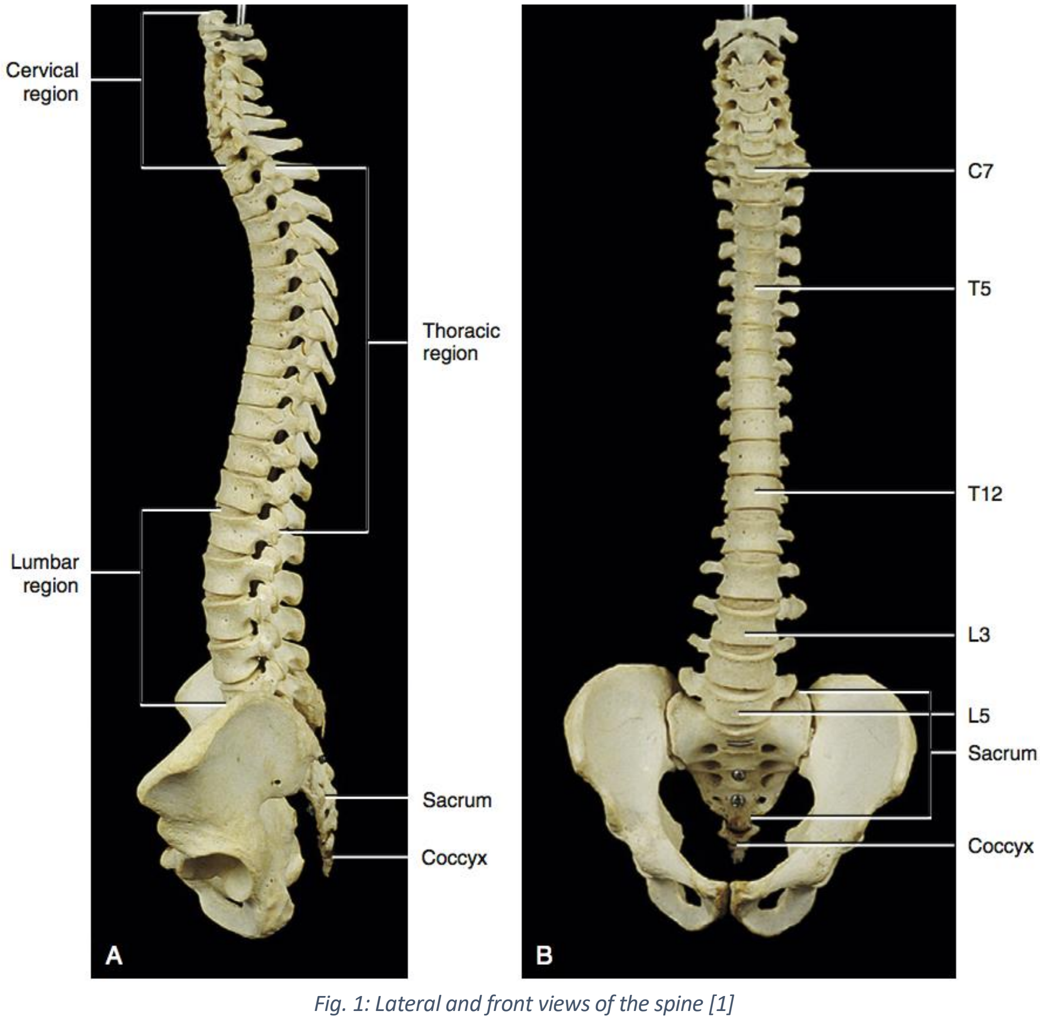

Fig. 1: Lateral and front views of the spine [1]

Vertebrae have two regions, a vertebral body and a vertebral arch (Fig. 2). The vertebral body is the cylindrical interior part of the vertebra and is responsible for holding the body weight. On the other hand, vertebral arch is constituted by pedicles, laminae, and superior articular, inferior articular, transverse and spinous processes; and is responsible for protecting the spinal cord (which lies inside the vertebral foramen, spinal canal). Bone in both regions has an outer layer of compact bone and a core of trabecular (cancellous) bone. In the cancellous bone region, vertical trabeculae predominate over horizontal ones. The reason for this is that trabeculae align themselves along the maximum stress direction, in this case, responding to axial loads. What's more, horizontal trabeculae serve as support elements for the vertical trabeculae and give stability to the bone (like beams in a building).

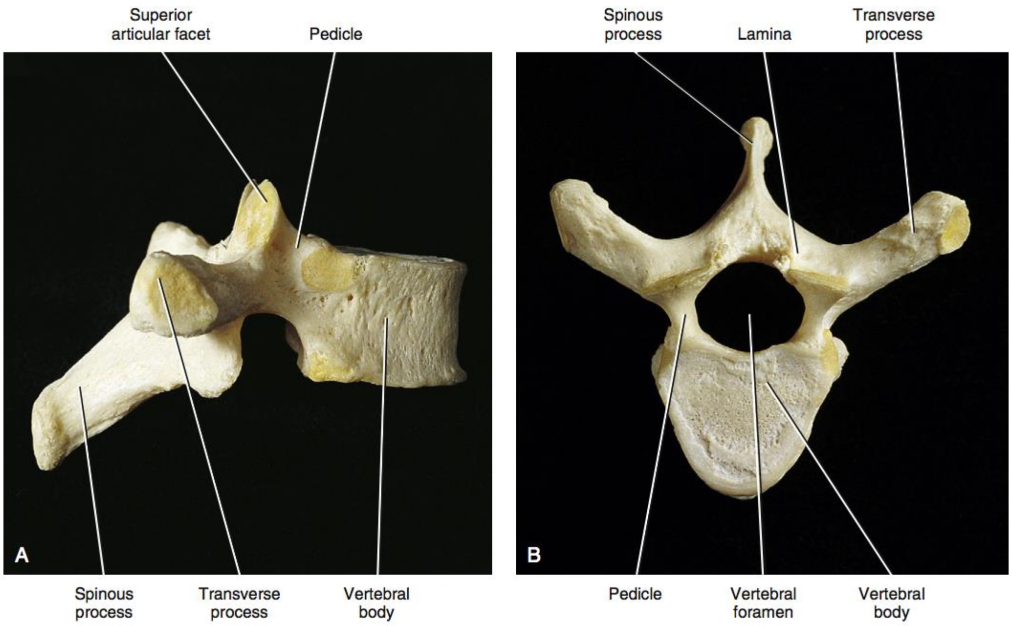

Fig. 2: Lateral and superior views of a thoracic vertebra [1]

Bony anatomy varies between the 4 regions into which the spine is divided. For instance, vertebral body suffers an increase of its transverse diameter from C2 to L3 (as can be seen in Fig. 1.B). This may be due to the fact that each vertebra has to hold more weight than the one above it. On the other hand, vertebral arch shows a more significant variation between different regions. In Fig. 3, the different shapes of the vertebral arch are shown.

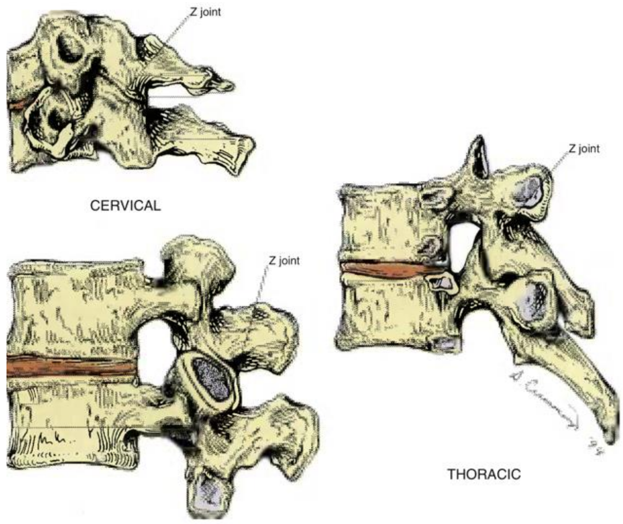

Fig. 3: Lateral views of the morphology, vertebrae have in different regions. [2]

Each one of the vertebrae that constitutes the spine is in contact with its neighbouring vertebrae through fibrocartilaginous intervertebral discs and articular facets (except for the sacrum, region where vertebrae are fused together). These intervertebral discs have a gelatinous core and are composed of a fibrotic ring with various concentric layers of collagen fibres. Their function is to serve as shock absorbers and avoid direct contact between neighbouring vertebral bodies.

Additionally, there is an intervertebral joint between each pair of vertebrae, formed by ligaments. The role of these ligaments is to allow smooth movement and to protect the spinal cord by limiting the maximum motion of the spine. An image of these ligaments can be seen in Fig.4.

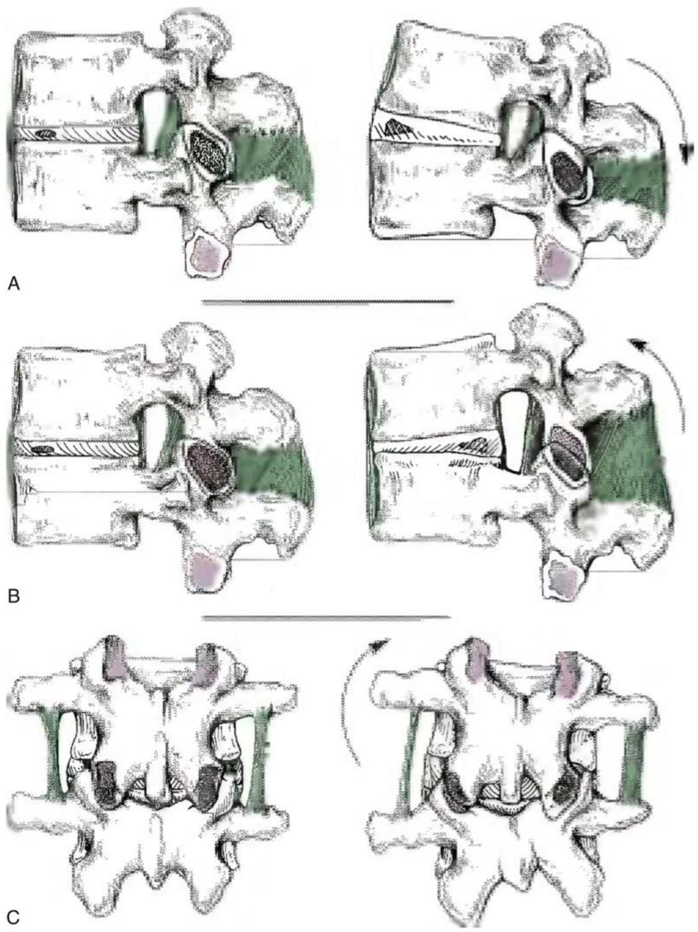

Fig. 4: Saggital (A, B) and posterior (C) view of vertebrae showing the functioning of ligaments when neighbouring vertebrae move. [1]

1.2. Spinal diseases

In this section, the spinal diseases shown by the patients who were selected for this study, are defined. Along with the factors than can be the cause for their appearance and the possible treatments used to heal them and relieve pain from the patient.

1.2.1. Compression Fractures

It is the fracture of the vertebral body of a vertebra due to excessive compression stress, which may be caused by a trauma. Vertebrae's structure is optimized to hold the weight of the trunk and the head. Thus, the trauma needed to break the bone of the vertebral body is considerably high. However, osteoporosis (a condition which can happen to elder people) causes the mass density of bone to decrease. Thus, making the bones more fragile, making it easier to be broken by a small impact.

Fig. 5: Lateral and anteroposterior X-ray showing an L1 compression fracture [WebPage: Medscape]

A nonsurgical treatment for compression fractures allows the pain to heal itself naturally with bed rest. However, physical activity periods should also be included in the treatment, so as to not worsen bone loss. On the other hand, if pain persists, surgical treatment is needed. This consists in injecting a bone cement mixture into the fractured vertebrae to restore mass density and volume of the fractured vertebra.

1.2.2. Spondylolisthesis

From the Greek words “spondyl” (spine) and “olisthesis” (slippage), it refers to the slippage of one vertebra and the spinal column above, on the vertebra below. Basically, due to the fact that there has been a problem with one of the joints that keep the vertebrae lined (i.e. injured ligaments or degenerated intervertebral discs). Thus, allowing neighbouring vertebrae to slip.

It can have many causes. Among them, we can find: a congenital defective joint, a joint that has been damaged by a trauma or has suffered too much stress, or the infection of a joint.

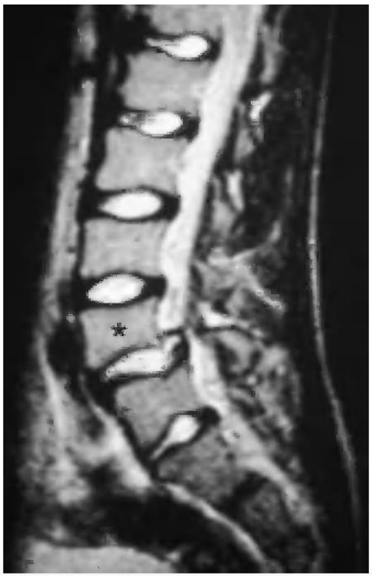

Fig. 6: Lumbar MRI showing spondylolisthesis of L4 in a 13-year-old boy [2]

Treatment for spondylolisthesis includes any action to prevent the cause of the slippage (i.e., weight loss on overweight people or core strengthening). In the event of movement still continuing, surgery must be done. In this case, elimination or fusion of bone is needed. Depending on whether it is needed to take a load off the affected region or to fuse the bones in their correct location.

1.2.3. Kyphoscoliosis

It is a disorder combining kyphosis (outward curvature of the spine) and scoliosis (associated with lateral bending of the spine). Among the factors that can cause it, we can find: keeping a bad posture for prolonged periods of time, structural changes due to osteoporosis and aging, traumatic injury which has led to the deformity of the spine and congenital disorder.

Fig. 7: X-ray showing scoliosis in a child, before and after instrumented fusion [1]

Nonsurgical treatment for Kyphoscoliosis consists in physical therapy when the spinal curvature is mild. On the other hand, when the deformity affects other physiological functions, surgical treatment is required. The correction consists in fixing the spine, stopping any further progression of the curvature.

1.2.4. Pseudarthrosis

It is called false joint and refers to the movement of bone at the location of a fracture due to a failed spine fusion. Fusion surgery is intended to weld two or more vertebrae into a solid piece (or one vertebra that has broken into various pieces). It sometimes even implies the use of bone graft to achieve a successful outcome. However, there is a risk of a non-successful outcome for this sort of surgery, and patients who smoke, with diabetes or with osteoporosis, have an increased risk of suffering pseudarthrosis after a fusion surgery.

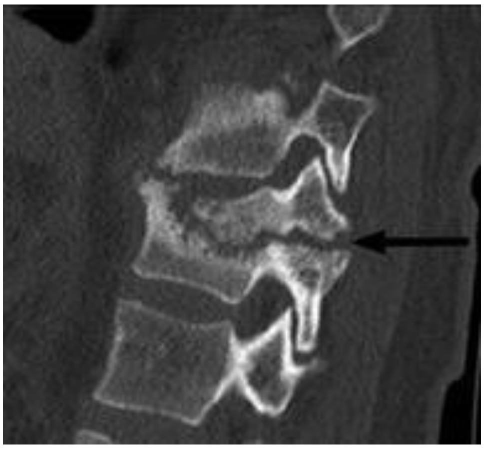

Fig. 8: CT image showing a T11 vertebra with pseudarthrosis [WebPage: ResearchGate]

Treatment for pseudarthrosis consists in a second attempt at fusion. That includes the use of bone graft substitutes or spinal instrumentation to fix the affected vertebrae.

1.2.5. Discopathy

It is the most common surgical disease of the spine and it refers to any disease that affects the intervertebral discs. It happens when the fibres in the fibrotic ring start breaking, and the ring structure is lost. The breakage of these fibres can be caused by multiple micro-trauma or by congenital disorders.

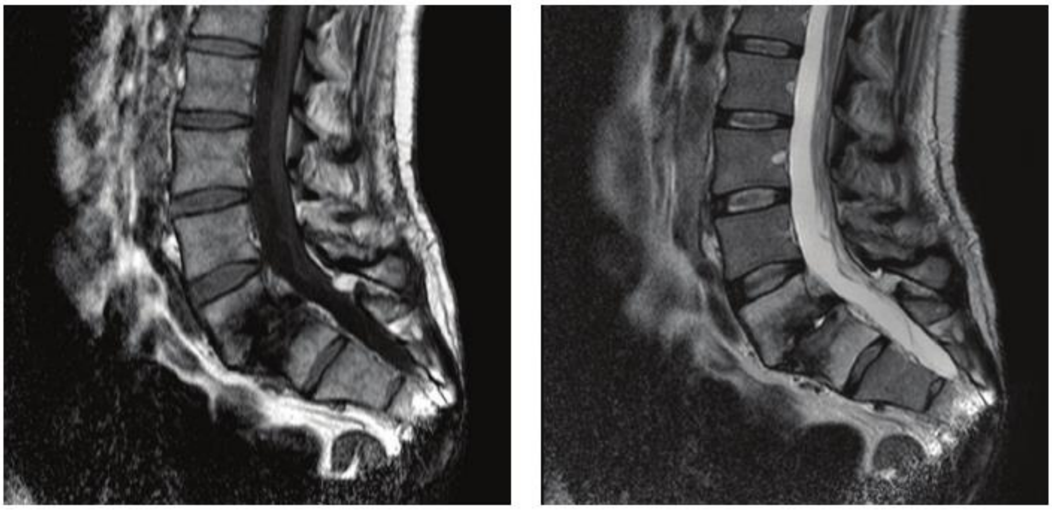

Fig. 9: MRI showing an L5/S1 with severe discopathy [Webpage: ResearchGate]

Nonsurgical treatment of discopathy consists in resting, combined with physical activity and back strengthening. If the patient does not respond favourably to conservative treatment, fusion surgery must be done. This reduces the pain by stopping the motion of the affected region.

1.2.6. Stenosis

It is the narrowing of the spinal canal. It can cause the spinal nerve roots or spinal cord to become pinched, needing decompression.

It can be caused by the compression of the spinal canal due to the accumulation of space-occupying degenerative material

Fig. 10: MRI showing L3-L4 compression of the spinal canal [Webpage: DanielParkMD]

As the width of the canal cannot be restored naturally over time, nonsurgical treatment of stenosis has the only goal of relieving pain. If stenosis causes the appearance of neurologic deficits, surgical procedure must be performed. The chosen procedure is decompressive laminectomy (surgery which creates space in the spinal canal by removing the lamina) of the affected region.

1.3. Imaging of the spine

Radiological assessment of the spine is essential for the investigation and treatment of spinal disorders. And there are several ways in which images of the spine can be obtained. Such include plain radiographs, fluoroscopy, myelography, bone scanning, computed tomography, magnetic resonance imaging. This section will be focused on the two used techniques in this project: Fluoroscopy and Computerized Tomography.

1.3.1. Fluoroscopy

Fluoroscopy is an imaging technique mainly used during the operation. It uses X-rays to obtain real-time images of the internal structures of your body (like a movie). Thanks to this, the physician can guide a needle into the appropriate area of the spine and be able to know at every moment the position of the needle or the pedicle screw inside the body. Thus, having a starting point for the pedicle screw as well as its position "during" the injection process.

The equipment required to perform fluoroscopy is that shown in Fig. 11. The C-arm allows the physician to get X-ray images of the patient from almost any angle.

Fig. 11: Fixed fluoroscopic System [Webpage: PeekMed]

1.3.2. Computerized tomography

It is an imaging technique that uses a rotating X-ray tube to provide cross-sectional images of a part of the body. The X-ray tube rotates along a donut-shaped structure (gantry, as shown in Fig. 12) while a patient table moves in a perpendicular direction. Each time the X-ray tube completes a rotation, a 2D image slice is built. Thus, this method allows contiguous slice acquisition and thanks to the advancement of computer graphics, it has gained a lot of popularity and acceptance when used for multi-planar reconstructions. It is used to diagnose injured patients. At the same time, it can be used to control, once the surgical procedure is finished, the outcome of the operation.

Computerized tomography has a remarkable advantage over other methods using X-ray (like plain radiographs). It allows to differentiate soft tissues as well as bone architecture. However, one of the drawbacks is the high ionizing radiation to which the patient is exposed.

Fig. 12: Computed tomography Scanner [Toshiba]

2. State of the art

Spine fusion surgery procedures using transpedicular fixation have risen in the last decades. The increase in life expectancy of modern society, where elderly population form an ever-greater proportion, is directly related to that trend [4-7]. Thus, the complications and outcome of this sort of surgery concerning elder people affected by severe degenerative spinal diseases and osteoporosis have become the topic of several investigations [8]. Additionally, complications during spine fusion procedures on lumbar and sacral vertebrae are more likely to appear on elderly patients than on any other sector of the population. And of special interest and relevance is the risk related to osteoporotic bone fixation [9-12]. For instance, a revision of the literature reveals a linear correlation between pull out strength of pedicle screws and bone mineral density [13, 14].

To reduce the overall impact of these complications, cement augmentation of pedicle screw fixation has become a widely-used technique for providing spine stability and correcting spinal deformity. It has been reported that this procedure can increase screw pull out strength by a factor of up to 1.5 compared to surgical procedures that employ non-augmented screws [15]. Such has been its contribution to surgical success, that, currently, it has become a commonly used implant in spinal surgery, providing superior spine stability in elderly patients with osteoporosis and various spinal diseases [16-21].

There have been many proposed approaches as to how the screw augmentation technique should be carried out. However, biomechanical test results seem to point to cemented polymethylmethacrylate (PMMA) augmentation as being the most effective method for improving the fixation strength of pedicle screws. In any case, there still are several factors that need to be taken into consideration if optimum spine stabilisation is to be achieved through this method. First, regulation of both, homogeneity and viscosity of the cement plays a fundamental role in assuring trabecular bone interdigitation and preventing any extra osseous cement leakage. Second, continuous control over the injection process is essential to avoid damaging surrounding regions close to the insertion position. And third, achieving symmetrical cement flow distribution around the pedicle screw has been recognised to improve screw fixation in vertebral body [16, 22-24].

There have been several studies assessing the increase in resistance to pull out and toggle failure in lumbar vertebrae yielded by the use of cement to augment pedicle screw fixation [8, 25]. Yet, very few studies have been able to acknowledge this effect in sacral (S1) vertebra. Furthermore, most of the studies published in the field of cement augmentation of pedicle screws are experimental and few clinical reports on the application of these techniques in clinical practice are available. And finally, by means of clinical experience, it has been seen that symmetrical cement distribution around the screws cannot always be obtained and it seems especially critical when treating lumbosacral vertebrae

3. Goal of the project

The purpose of the present study is to analyse clinical cases to quantify - with the help of a new Computer Aided Design (CAD) approach - the distribution of PMMA injected cement in lumbar (L4 and L5) and sacral (S1) vertebrae in elderly patients with poor bone quality. With a view to build a strong knowledge of cement behaviour in these vertebrae and assure screw fixation in these regions.

4. Materials and Methods

4.1. Study design

A total of 37 patients (27 females and 10 males, mean age 76 years, range 55-89 years) with low bone mineral density and various spinal diseases were selected for this project. They underwent spinal instrumentation with cement augmented pedicle screws.

As an overview of the spinal diseases shown by the patients, 1 patient suffered from compression fractures; 11 patients suffered from lumbar spondylolisthesis; 17 patients suffered from kyphoscoliosis; 1 patient suffered from kyphosis at the adjacent level with pseudarthrosis at previously fused level; 4 patients suffered from degenerative or adjacent discopathy and 3 patients suffered from lumbar stenosis. They underwent a standard, open, posterior midline approach to the lumbar spine. Patients with foraminal or central canal stenosis requiring aggressive decompression underwent laminectomy prior to fusion using cannulated cemented pedicle screw instrumentation. All patients were first examined through dual energy X-ray absorptiometry (DEXA). A mean T-score[1] of -2,27 (-4,4 to 1) was obtained, indicating bone density below normal, leading to osteopenia to severe osteoporosis.

The lumbosacral spine levels evaluated in the present work were located as follows: L4-L5 for 13 patients, L4-S1 for 15 patients and L5-S1 for 9 patients.

4.2. Surgical procedure

Each vertebra was treated bilaterally using cannulated fenestrated pedicle screws (Omega21™, Biomet® Inc., Indiana, USA), and with the same augmentation technique as the other vertebrae, using vertebroplasty cement (Biomet V, Biomet® Inc., Indiana, USA). The cannulated fenestrated pedicle screws (with a diameter of 6.35 mm) had a central canal without a distal opening and 2 small and 2 large holes located at 12 and 25 mm length from the tip. In the case of lumbar vertebrae (i.e. L4 and L5) 50 or 55 mm-length pedicle screws were used, while in the case of S1 vertebra 40 or 45 mm-length pedicle screws were chosen. The maximum quantity of injected cement per screw was limited to 3 ml for all cases.

[1] Patient's bone density compared to what is expected in a young adult of the same sex, which can vary from -4,4 to 1.

The pedicle screws placement and cementation was carried out under C-arm fluoroscopy. This intraoperative monitoring technique helped to locate the optimal starting pedicle point for screws and to check the hole through the pedicle created by the pedicle finder. It also contributed in controlling the angulation and position against the anterior vertebral wall of the inserted pedicle screws as well as controlling the distribution of the cement and any possible leakage. The placement of all screws was performed after removing the cortical bone at the pedicle entry site. After having created the hole, a standard rounded pedicle finder was guided with the help of fluoroscopy, so that its tip did not go beyond 1/3 of the vertebral body. Then, a palpation of the bony wall was performed in order to check if the pedicle wall and the cortex of the vertebral body were intact. After that, it was taped with a 5.5 mm tape.

Once all cannulated pedicle screws were inserted with concentric angulation and checked for correct positioning, the instrumentation was completed and the screws were dynamometrical tightened. The cement was mixed and apportioned among three 1-cm^3 sterile syringes (3 cm^3). These syringes fit in the screw's head and allowed for fine control over the flow of cement. When the cement reached a tooth paste-like viscosity, it was slowly injected through the screw. This operation proceeded under the same control measures as standard vertebroplasty. That is, continuous fluoroscopy so as to keep control of the distribution of the cement and any possible leakage. In case of leakage, cement injection was stopped and resumed a short time later. Fig. 13 shows some pictures of the clinical procedure and its outcome.

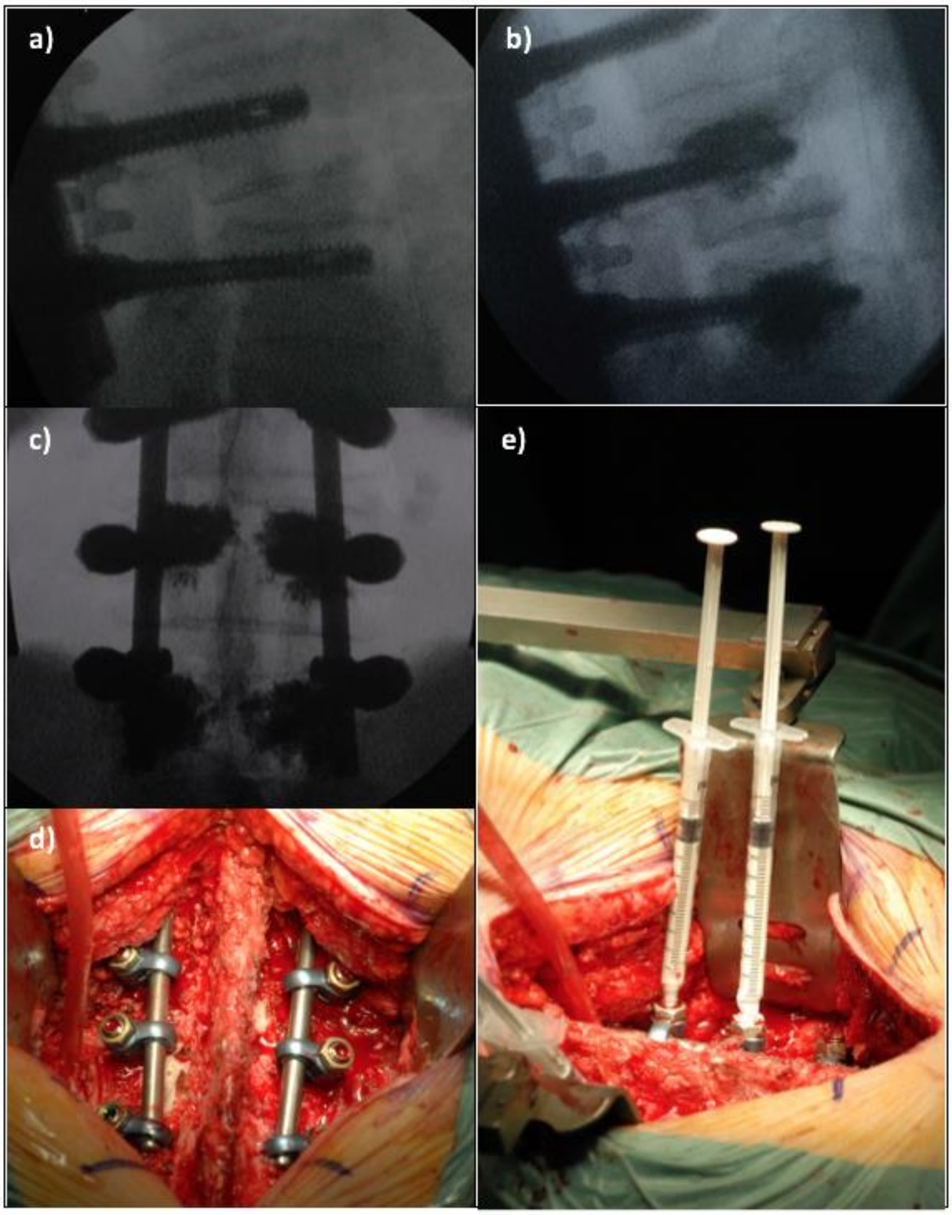

Fig. 13: Some steps of the surgical procedure: a) Pedicle screws placed in position prior to cementation. b) and c) Injection of bone cement under continuous fluoroscopy control. d) and e) Final surgery outcome before and after putting in place the 1 cm^3 syringes for bone cement injection.

4.3. Postoperative analysis

4.3.1. 3D model reconstruction

A dual-energy multidetector CT scanner (Somatom Definition Flash, Siemens Medical Systems, Germany; 128x2 slices, layer thickness of 1.0 mm, dual voltage of 80 and 140 kVp, current of 203 and 80mAs, CareDose 4D, and acquisition 32x0.6mm) was used to monitor the patients once 6 months had passed after the operation. The CT files, in DICOM format, were imported to Invesalius 3.0 open source software (http://www.cti.gov.br/invesalius/) for the three-dimensional (3D) reconstruction of the computed tomography images (see Figs. 14.a-c). Before the 3D virtual reconstruction, images were treated with automated tools for noise reduction, smoothing and segmentation.

4.3.2. Data acquisition

The 3D models showing the isolated screws and surrounding cement (see Fig. 14.c) were then exported directly to Rhinoceros 3D© software (Robert McNeell & Associates, v.4.0 SR9) as STL (Stereo Lithography) files (see Fig. 14.d) in order to study bone cement distribution around each individual screw (see Fig. 14.e). From that point, the *Rotate* software command was used to conveniently orient each screw (see Fig. 14.f) as to obtain the maximum longitudinal (see. Fig. 14.g) and transversal (see Fig. 14.h) 2D cement profile projections. Then, the *MeshOutline* software command was used to create a polyline outline-profile of the polygon mesh objects for the projected surfaces (see also Fig. 14.f). Finally, the *AreaCentroid* software command reported for each specific polyline profile the Cartesian coordinates of its centroid. That is, the average mass centre point of the bone cement distributed around the cannulated and fenestrated pedicle screws. Thus, providing an approximation about the quantity of bone cement that achieved a symmetric distribution around the screws. All the data of the centroids are included in Table 1.

Once the centroids of the various profiles had been obtained, statistical analysis comparing the cement's behaviour between different vertebrae and pedicle screws were performed. The analysis was performed with Minitab Statistical Software. The sort of analysis being, an ANalysis Of Variance.

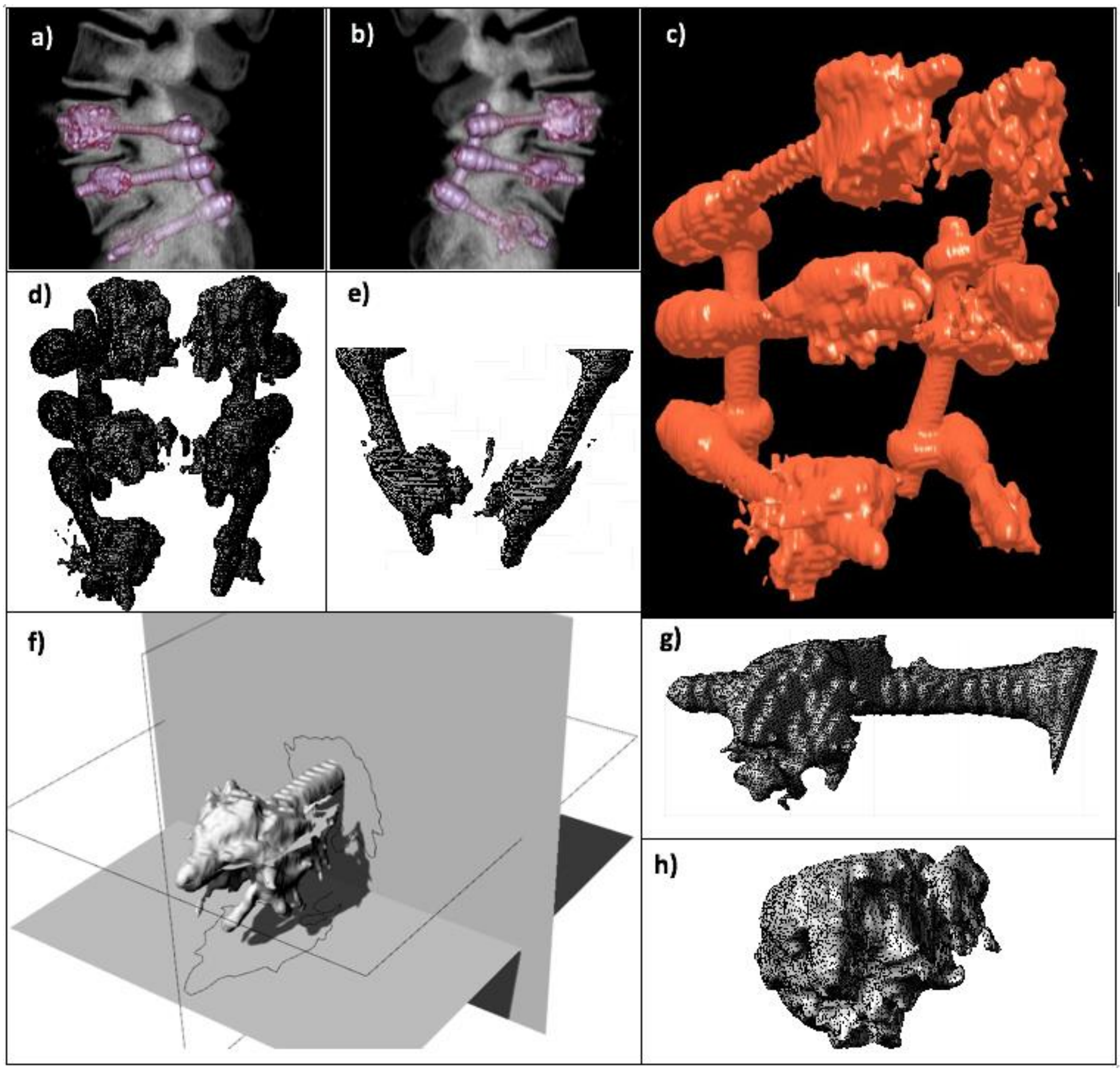

Fig. 14: Experimental process followed to obtain the maximum sagittal and axial bone cement flow profiles around the spine screws: a) and b) 3D reconstruction of bone cement surrounding the screws in L4, L5 and S1 vertebrae (done with free open software InVesalius 3.0). c) 3D isolated model for the screws and the surrounding cement. d) 3D reconstructed model exported to Rhinoceros© 3D in STL format. e) Isolated 3D models for each screw. f) CAD model and method used to obtain the maximum longitudinal and transversal 2D flow cement profiles. g) CAD model showing the longitudinal 3D distribution of bone cement. h) The same as before but for a transversal view.

5. Results

As explained in section 3.2, Fig. 14.f, which is the starting point for further data processing, shows a reconstructed CAD model of the pedicle screw with the injected cement, together with the Cranium-Caudal longitudinal and the Antero-Posterior transversal 2D-projected views of the maximum cement profiles. In this sense, Fig. 15 shows a set of these profiles (P) obtained for the pedicle screws inserted into the L4, L5 and S1 vertebrae of the same patient. It can be noticed that the main differences between pedicle screws inserted in separate vertebrae have strongly emerged when examining the transversal plots (see, Fig. 15.c and 15.d). On the contrary, the longitudinal views (see Fig. 15.a and 15.b) haven't shown such variation.

To better account for these differences, the centroid (C) polar coordinates of the profiles have been additionally plotted. These centre points allow for better visual differentiation between cement injected in different screws. For example, for a longitudinal view, Fig. 15.a and 15.b while showing no significant differences between the L4, L5 and S1 vertebrae, i.e. the centroids nearly coincide, they do show an average tendency of the centroids to deviate towards the inner central part of the vertebra for both, the right (Fig. 15.a) and the left (Fig. 15.b) screws. This tendency is also captured by the transversal view (see, Fig. 15.c and 15.d), which accounts for better differentiation between vertebrae. For that patient, the cement in the right screw deviates towards the centre-down and the centre-top part of the L4 and L5 vertebrae, respectively. While cement injected in the right screw of S1 vertebra shows a more symmetric distribution. On the other hand, for the left screws, the cement injected in the S1 vertebra clearly deviates towards its downright wall, displaying a high asymmetrical distribution compared to a more symmetrical cement distribution shown by L4 and L5 vertebrae.

Table 1: X and Y coordinates of the centroid points obtained for the whole set of studied pedicle screws. Differentiating between vertebrae (L4, L5 and S1) and pedicle screw (Right and Left)

L4 Right		**L4 Left**		**L5 Left**		**L5 Left**		**S1 Right**		**S1 Left**	
X	**Y**	**X**	**Y**	**X**	**Y**	**X**	**Y**	**X**	**Y**	**X**	**Y**
-0,85	-0,39	1,09	-1,39	0,5	1,14	-1,01	-1,21	-5,22	-1,8	3,21	0,64
0,79	-2,65	0,55	-4,59	2,46	0,49	3,03	-4,37	-0,64	-2,95	3,84	-3,16
3,31	0,04	1,36	-3,14	0,17	-2,9	0,62	-2,67	2,38	2,39	-3,22	-2,41
-3,59	-1,71	-0,67	-1,24	1,73	-0,46	-0,78	-2,21	2,59	0,29	1,13	-2,11
-4,15	-6,07	1,85	-1,53	1,7	0,33	-2,32	-0,81	-0,64	-1,84	1,15	-3,29
1,73	-2,24	-1,01	0,54	3,55	2,36	-1,5	1,39	4,07	-1,62	-4,56	-3,4
3,03	-1,18	1,59	1,56	1,41	-1,52	1,76	0,12	-4,34	-2,54	0,41	-2,43
0,97	-1,33	1,68	-2,14	3,7	-4,2	-2,93	0,49	-3,9	-1,01	-0,24	-2,47
3,80	-3,15	1,27	-4,43	-2,85	-5,95	2,09	1,96	-0,26	-4,1	2,75	-5,64
0,09	-1,22	1,54	-4,62	3,62	-4,22	-3,12	-2,28	-0,65	-3,51	1,84	-2,89
0,05	-4,95	-1,84	0,56	4,09	-2,83	-3,08	-1,16	0,35	4,34	1,16	0,6
-4,00	1,39	-0,29	-2,08	4,43	1,41	-1,36	-0,05	-3,23	-4,25	0,56	-6,65
4,48	-0,03	-1,24	-3,17	6,19	-1,65	-2,11	-3,64	-2,08	-7,05	4,66	-3,95
0,66	-2,82	-1,1	-2,79	0,38	-2,52	-4,69	4,6	0,78	-1,99	0,04	-1,7
1,44	0,02	-1,85	-1,6	2,05	-1,95	3,32	0,68	6,5	-3,84	4,45	-1,21
-1,81	0,04	-2,96	0,34	-1,75	-0,42	-4,1	2,14	-4,32	-0,35	3,12	-5,75
3,92	-0,14	-3,94	0,17	-1,05	-0,22	-4,72	2,55	-3,57	-2,69	-0,93	-5,98
0,55	-0,53	-3,27	-1,13	-0,26	0,21	-2,29	0,19	1,14	-5,42	-0,9	-3,51
3,22	3,57	1,21	-1,76	-0,17	-2,24	-0,97	2,16	5,35	-2,89	1,59	-1,49
0,54	-2,95	1,96	-0,32	1,53	2,53	-0,83	-1,21	-2,19	2,43	1,87	0
0,47	-1,03	1,29	2,47	-0,24	-0,93	-0,31	-0,25	0,14	-1,43		
5,57	1,31	2,25	1,97	0,19	4,42	-4,79	1,08				
0,13	0,71	-0,08	1,22	2,55	1,42	-1,4	1,77				
1,58	-2,79	2,42	-2,44	1,64	-1,65	-0,98	-0,93				
1,60	-1,15	2,05	0,62								
2,05	1,08	0,54	0,04								
-0,39	-4,02	4,72	-0,82								
0,05	-4,13										

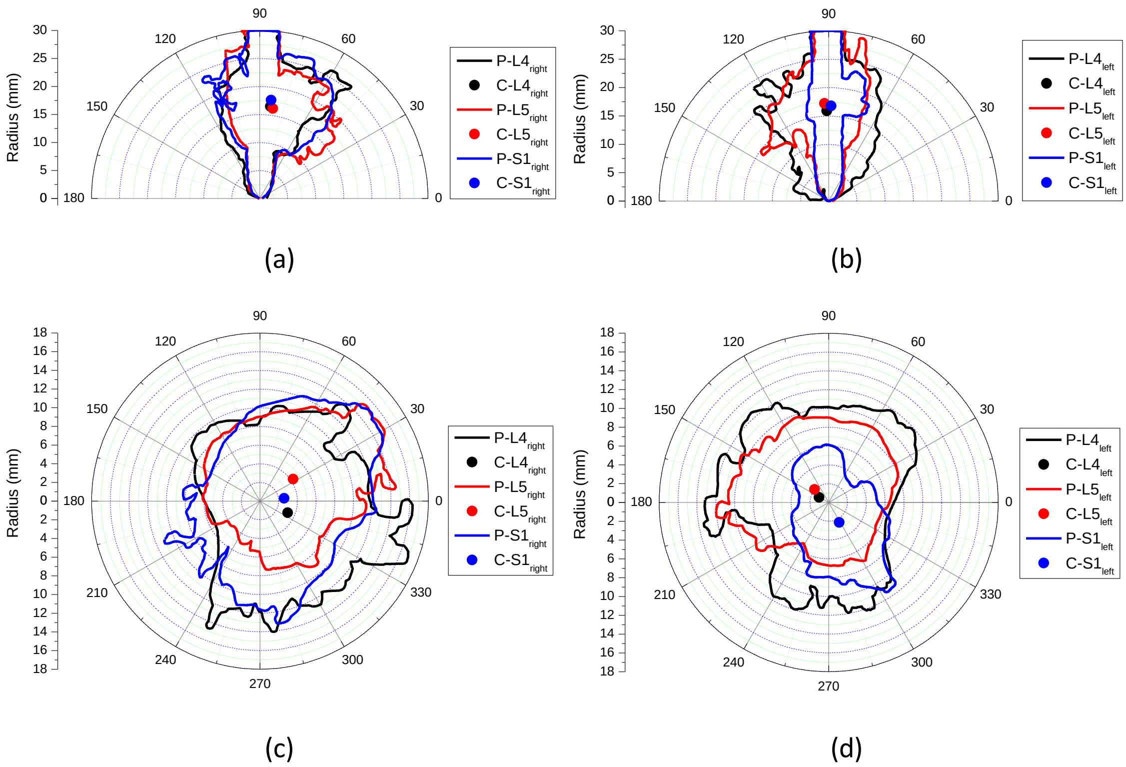

Fig. 15: Representation in polar coordinates of cement profiles (P) and centroids (C) measured around spine screws inserted into the L4, L5 and S1 vertebrae of the same patient. (a) Cranium-Caudal (CC) longitudinal view of the right screws. (b) CC longitudinal view of the left screws. (c) Antero-Posterior (AP) transversal view of the right screws. (d) AP transversal view of the left screws.

Fig. 16 is a graphic depiction of all the centroid coordinates obtained for the complete set of analysed vertebrae of the patients and intends to clarify the above-mentioned particular observations. This figure allows for a proper study of cement distribution differentiating between both, the right and the left screw insertion positions, and the different vertebrae (L4, L5 and S1). The figure presents the centroids of its corresponding longitudinal view of the maximum cement profile (see also Fig. 15). In it, the similarity in performance between pedicle screws inserted into the L4, L5 and S1 vertebrae can be seen. For example, Figs. 16.a-c show no significant differences between the average centroid points of both, the right and the left screw cement profiles in the L4, L5 and S1 vertebrae, respectively. Additionally, the average centroid points are aligned between the polar coordinates of radius 15-20 mm and 0º, which are at half way the maximum longitudinal size of the screw considered (30 mm) and along the symmetric longitudinal axes of the same.

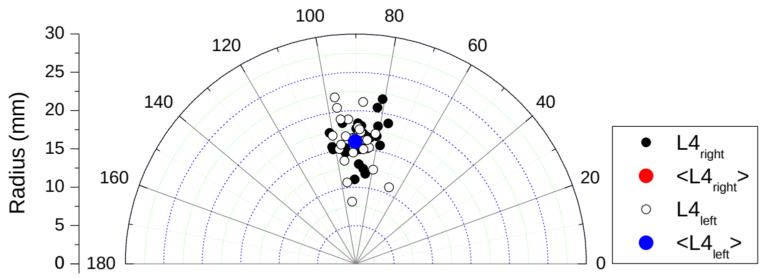

(a)

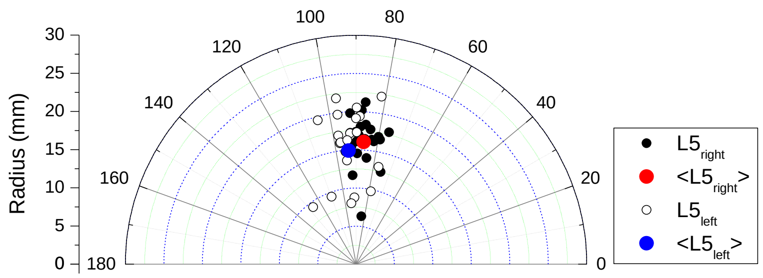

(b)

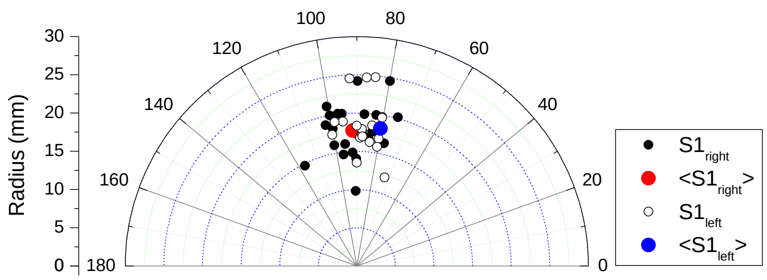

(c)

Fig. 16: Representation in polar coordinates of all the centroid points measured for the corresponding longitudinal cement profiles surrounding the spine screws inserted, right and left, into the L4 (a), L5 (b) and S1 (c) vertebrae of the population under study. Centroid average values for the right and the left series are also indicated.

Similarly, Figure 17 depicts the centroids corresponding to the transversal view of the maximum cement profiles. In this figure, the variation between the behaviour of the injected cement into the separate vertebrae materializes. For example, Fig. 17.a shows that for the L4 vertebra the right screws concentrated the cement to the centre-down part of the vertebra (average centroid being at the fourth quadrant) while left screws did it to the left-down wall of the same (average centroid also at the fourth quadrant). The average Cartesian coordinates and the standard deviations (x_{right}(±StD_{xright}), x_{left}(±StD_{xleft})) – (y_{right}(±StD_{yright}), y_{left}(±StD_{yleft})) corresponding to the transversal average centroid points for the L4 vertebra were (0,90 (±2,40), 0,34 (±2,00)) mm – (-1,30 (±2,13), -1,10 (±1,97)) mm. Despite this observation, statistical analysis of the data through a one-factor ANOVA showed no statistically significant difference between the mean values of the Cartesian coordinates of the centroids of both screws ($p>0,05$).

On the other hand, Fig. 17.b shows that for the L5 vertebra both, right and left screws deviated cement to the corresponding centre of the vertebra (the average Cartesian coordinates and standard deviations of the centroids of the transversal plots being: (1,48 (±2,12), -1,35 (±2,30)) mm – (-0,81 (±2,41), -0,07 (±2,12)) mm. Thus, the one-factor ANOVA confirmed this observation by showing only a statistically significant difference between the mean values of "x" coordinates ($p<0,05$). As a result, the average centroid points of both, right and left screws nearly coincide with the polar origin coordinate (see red dot).

Additionally, Fig. 17.c shows that cement injection into the S1 vertebra displayed a quite different behaviour. In this case, both screws (right and left) significantly deviated the injected cement to the corresponding downside walls of the vertebra (note the position of the corresponding centroid points). The average Cartesian coordinates and the standard deviations of the centroids of the transversal profiles being: (-0,37 (±3,26), 1,10 (±2,37)) mm – (-1,90 (±2,67), -2,84 (±2,08)) mm. The one-factor ANOVA showed no statistically significant difference between the behaviour of injected cement in the different screws ($p>0,05$).

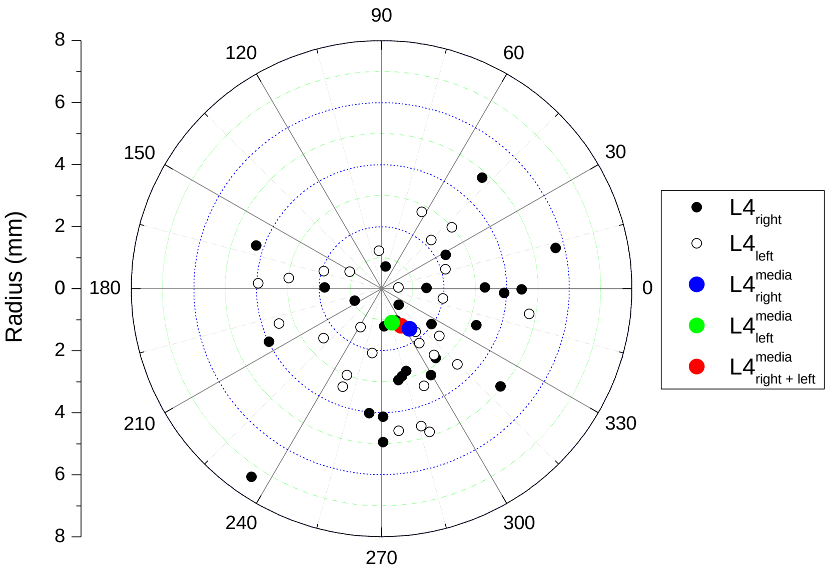

90
60
30
0
330
300
270
240
210
180
150
120
Radius (mm)
8
6
4
2
0
2
4
6
8
L4 right
L4 left
L4 media right
L4 media left
L4 media right + left

(a)

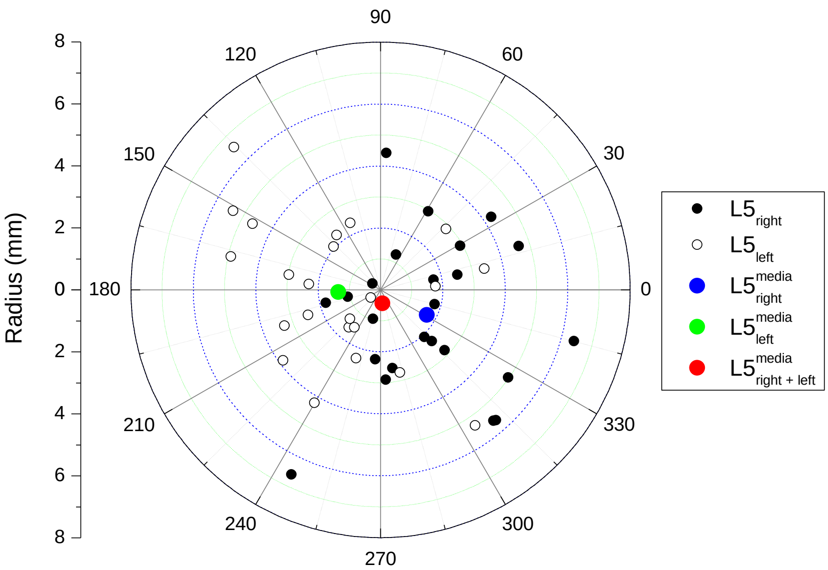

90
60
30
0
330
300
270
240
210
180
150
120
Radius (mm)
8
6
4
2
0
2
4
6
8
L5 right
L5 left
L5 media right
L5 media left
L5 media right + left

(b)

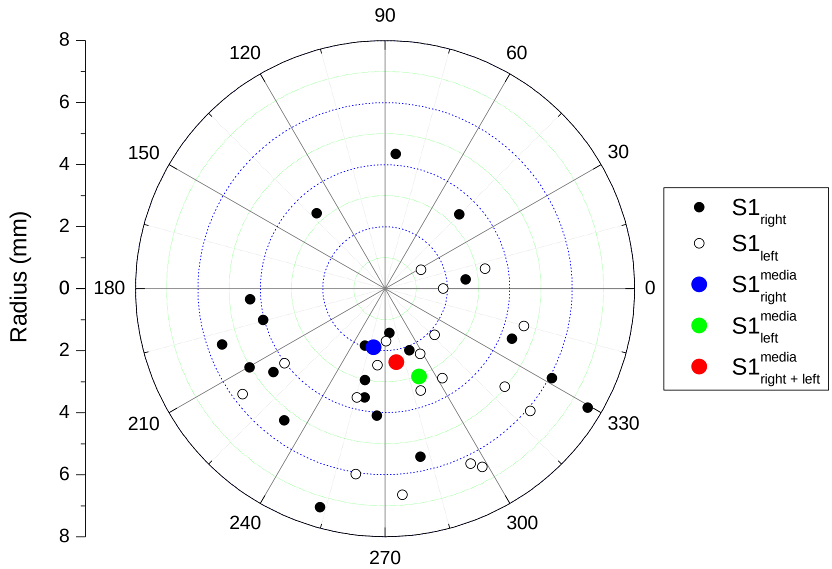

(c)

Fig. 17: Representation in polar coordinates of all the centroid points measured for the corresponding transversal cement profiles surrounding the spine screws inserted, right and left, into the L4 (a), L5 (b) and S1 (c) vertebrae of the population under study. Centroid average values for the right, the left, and both together series are also indicated.

Lastly, the results obtained for the S1 vertebra are a clear indicator that cement injected into sacral S1 vertebra behaves differently from lumbar L4 and L5 vertebrae. While in lumbar vertebrae the cement mainly distributes symmetrically around the screws, in the sacral vertebra, symmetric and homogeneous cement distribution is not assured and so is not its fixation.

These observations were further confirmed by another statistical analysis of the data. The average Cartesian coordinates and the standard deviations (x(±StD_x), y(±StD_y)) corresponding to the transversal average centroid points of joined «right+left» data populations (see red dots in Fig. 17) were as follows: a) for the L4 vertebra, (0.62 (±2.21), -1.20 (±2.03)); b) for the L5 vertebra, (0,06 (±2,62), -0,44 (±2,27)); and c) for the S1 vertebra, (0,36 (±2,92), -2,37 (±2,42)). The one-factor ANOVA analysis performed for the L4, L5 and the S1 series, in Cartesian coordinates, only showed a statistically significant difference between the mean values of “y” coordinates of S1 vertebra from L4 and L5 vertebrae. Thus, a statistical analysis of the average value of the radius was performed. The mean values and standard deviation of radius of joined populations were as follows: a) for the L4 vertebra (2,95 (±1,42)) mm; b) for the L5 vertebra (3,03 (±1,64)) mm; and c) for the S1 vertebra (4,49 (±2,19)) mm. At the light of these results, the one-factor ANOVA clearly indicated that the S1 vertebra showed a statistically significant different ($p<0,05$) behaviour as compared to the L4 and the L5 series. Additionally, the L4 and the L5 series did not show any statistical significance between them ($p>0,05$).

6. Discussion

Succeeding in achieving a reliable fixation of the pedicle screw in vertebral body has been, and will be, the key element in assuring a successful outcome of vertebroplasty. In this sense, PMMA cement augmentation has been proved to enhance pedicle screw fixation in osteoporotic lumbar vertebral body [19, 26-29]. Several studies have evaluated the improvement in pedicle screw fixation in osteoporotic bone caused by the cement augmentation technique [18-20, 23]. However, very few of them have carried out a comparison between lumbar and sacral vertebrae [30]. The goal of this sort of surgery is to achieve a homogeneous distribution in order to assure a better fixation of the pedicle screws into the vertebra, and this study has allowed us to notice the existence of differences in behaviour between PMMA cement distribution in lumbar and sacral vertebrae.

In this study, it was seen that PMMA injected cement distributed more uniformly around the inserted screws in lumbar (L4 and L5) vertebrae than in the case of sacral (S1) vertebra (see, Fig. 15). As seen in Fig. 16, centroids of the injected cement profiles into the lumbar region are located close to the central point of the vertebral body. This helps achieving a better fixation of the pedicle screw by allowing the screw to have the same amount of cement in every direction around it. Thus, avoiding any move or shift from its original position caused by the loosening of the screw. This performance behaves in agreement with the expected clinical outcome, where cement should fill the centre of the vertebra, avoiding approaching the walls.

On the contrary, centroids of the profiles of injected cement into the sacral vertebra (S1) show a scattered distribution, displaying a preferential flow of the cement to the lateral walls of the vertebral body. This leads to the possibility that injected cement found a preferential path towards the lateral walls instead of staying in the surroundings of the screw. The reasons for this are not yet clear but could be because of the fracture of weak trabeculae due to osteoporosis or high injection pressure, the existence of big cavities where cement finds no opposition to its flow, or the position of the screw. That last cause, i.e. the proximity of the screw to the lateral wall of the vertebra, could be affecting the eccentric distribution of cement in the sacral vertebra in a more visible way than in lumbar vertebra (see, Fig. 17). Furthermore, there are many other physical factors that affect the final distribution of PMMA cement augmentation and, consequently, affect the final fixation strength of pedicle screws. Such factors include the screw pitch and diameter, the quantity of openings for cement ejection and its distribution along the screw [29-36]. Considering these results, a permeability study of sacral vertebra (S1) will be necessary in order to learn the cause for this difference in behaviour shown by this vertebra.

On the other hand, when comparing cement distribution between L4 and L5 vertebrae, while showing a very similar behaviour, it can be seen in Fig. 17 that, on average, cement injected in L5 vertebra shows a centroid located very close the inner middle zone. Thus, leading to the possibility that pedicle screws inserted in L5 vertebra could show the most reliable performance after the bone cement filling injection.

At the light of our results, it appears clear that an improved fenestrated screw design would allow for a proper distribution in S1 vertebra. Improvements should help PMMA cement flow homogenously around the screw to assure its fixation, avoiding concentrating next to the lateral wall. In our opinion, this phenomenon will likely need more characterization implying a variety of different screws with openings in the distal region to ensure the achievement of a homogeneous distribution. On the other hand, we also think that the structure of cancellous bone in sacral vertebra affects the correct distribution of PMMA during its infiltration. Thus, making it necessary to study its behaviour with Computer Fluid Dynamic simulation (CFD) or real infiltration in cadaveric samples.

Finally, we hope that the results achieved in this study through the use of a novel CAD software technique will help build a better understanding about the behaviour shown by the injected cement into different vertebrae and contribute in improving augmentation techniques that are currently in use.

7. Conclusions

From all the results, three main conclusions can be drawn:

1) PMMA cement distributes homogeneously around spine-cannulated pedicle screws in lumbar vertebrae (L4 and L5) and consequently their fixation is assured.

2) PMMA cement does not distribute uniformly around spine-cannulated pedicle screws in sacra vertebra (S1) and consequently their fixation is not assured. In this case, the cement flows eccentrically to the superior and lateral walls of the vertebral body.

3) To improve the fixation in sacra vertebra (S1), PMMA cement should flow to the inner part of the vertebral body and distribute evenly around spine-cannulated pedicle screws. Screws currently in use do not have the capacity to confine cement placement because of their geometric openings. This means that new sacra screw designs are becoming necessary.

Environmental impact

All the work done in this project has only implied the use of a Workstation and a Computer. So, there has been no environmental impact during the realization of this project but for the consumed electricity.

Budget

Table 2: Cost overview of the project. Including personnel costs (Junior Engineer) and costs related with the use of Hardware (Workstation) and Software (Office 2016 and Grasshopper).

Budget		**Cost**	**Time**	**TOTAL (€)**
Personnel	Junior Engineer	20€/h	350 hours	7000€
Hardware	PC	6000€	5 months	500€
Software	Office 2016	150€	5 months	21€
	Grasshopper	500€	5 months	70€
TOTAL				7591€

Costs associated with software have been calculated from the license cost assuming it is expected to be in use for 3 years. The same applies to Hardware. The Workstation with which I have been working is expected to last 5 years.

References

1. D Skyrme Andrew, PF Selmon Guy, Apthorp Leslie (2005). Common spinal disorders explained. Remedica explained series. Remedica

2. D. Cramer Gregory, A. Darby Susan (2005). Clinical Anatomy of the Spine, Spinal Cord and Ans. Elsevier

3. Tay BKB, et al. (2014). Disorders, diseases, and injuries of the spine. In HB Skinner, PJ McMahon, eds., Current Diagnosis and Treatment in Orthopedics, 5th ed., pp. 156-229. New York: McGraw-Hill.

4. Piñera AR, Duran C, Lopez B, et al. Instrumented lumbar arthrodesis in elderly patients: prospective study using cannulated cemented pedicle screw instrumentation. *Eur Spine J* 2011;20(Suppl 3):408-14. doi:10.1007/s00586-011-1907-2

5. Recommendation CM/Rec (2009)6 of the Committee of Ministers to member states on ageing and disability in the 21st century: sustainable frameworks to enable greater quality of life in an inclusive society (Adopted by the Committee of Ministers on 8 July 2009 at the 1063rd meeting of the Ministers' Deputies).
https://rm.coe.int/CoERMPublicCommonSearchServices/DisplayDCTMContent?documentId=09000016806992fc

6. Rajaee SS, Bae HW, Kanim LE, Delamarter RB. Spinal fusion in the United States: analysis of trends from 1998 to 2008. *Spine* 2012;37(1):67-76. doi: 10.1097/BRS.0b013e31820cccfb.

7. Bederman SS, Coyte PC, Kreder HJ, et al. Who's in the driver's seat? The influence of patient and physician enthusiasm on regional variation in degenerative lumbar spinal surgery: a population-based study. *Spine* 2011;36(6):481–89. doi: 10.1097/BRS.0b013e3181d25e6f.

8. Elder BD, Lo SF, Holmes C, et al. The biomechanics of pedicle screw augmentation with cement. *Spine J* 2015;15(6):1432-45. doi: 10.1016/j.spinee.2015.03.016.

9. Li G, Patil CG, Lad SP, et al. Effects of age and comorbidities on complication rates and adverse outcomes after lumbar laminectomy in elderly patients. *Spine* 2008;33(11):1250–5. doi: 10.1097/BRS.0b013e3181714a44.

10. Raffo CS, Lauerman WC. Predicting morbidity and mortality of lumbar spine arthrodesis in patients in their ninth decade. *Spine* 2006;31(1):99–103. doi: 10.1097/01.brs.0000192678.25586.e5.

11. Daubs MD, Lenke LG, Cheh G, et al. Adult spinal deformity surgery: complications and outcomes in patients over age 60. *Spine* 2007;32(20):2238–44. doi: 10.1097/BRS.0b013e31814cf24a.

12. Esses SI, Sachs BL, Dreyzin V. Complications associated with the technique of pedicle screw fixation. A selected survey of ABS members. *Spine* 1993;18(15):2231–9.

13. Polly DW, Orchowski JR, Ellenbogen RG. Revision pedicle screws. Bigger, longer shims—what is best? *Spine* 1998;23(12):1374–9.

14. von Strempel A, Kühle J, Plitz W. Stability of pedicle screws. 2: Maximum pullout force with reference to bone density. *Z Orthop Ihre Grenzgeb*. 1994;132(1):82–6.

15. Wang W, Baran GR, Garg H, et al. The benefits of cement augmentation of pedicle screw fixation are increased in osteoporotic bone: a finite element analysis. *Spine Deformity* 2014;2(4):248-59. doi: 10.1016/j.jspd.2014.03.002.

16. Wittenberg RH, Lee KS, Shea M, et al. Effect of screw diameter, insertion technique, and bone cement augmentation of pedicular screw fixation strength. *Clin Orthop Relat Res* 1993;296:278–87.

17. Pfeifer BA, Krag MH, Johnson C. Repair of failed transpedicle screw fixation. A biomechanical study comparing polymethylmethacrylate, milled bone, and matchstick bone reconstruction. *Spine* 1994;19(3):350–3.

18. Tan JS, Kwon BK, Dvorak MF, et al. Pedicle screw motion in the osteoporotic spine after augmentation with laminar hooks, sublaminar wires, or calcium phosphate cement: a comparative analysis. *Spine* 2004;29(16):1723–30.

19. Renner SM, Lim TH, Kim WJ, et al. Augmentation of pedicle screw fixation strength using an injectable calcium phosphate cement as a function of injection timing and method. *Spine* 2004;29(11): E212–6.

20. Yi X, Wang Y, Lu H, Li C, Zhu T. Augmentation of pedicle screw fixation strength using an injectable calcium sulphate cement: an in vivo study. *Spine* 2008;33(23):2503–9. doi: 10.1097/BRS.0b013e318184e750.

21. Liu D, Wu ZX, Pan XM, et al. Biomechanical comparison of different techniques in primary spinal surgery in osteoporotic cadaveric lumbar vertebrae: expansive pedicle screw versus polymethylmethacrylate-augmented pedicle screw. *Arch Orthop Trauma Surg* 2011;131(9):1227-32. doi: 10.1007/s00402-011-1290-9.

22. Chang MC, Liu CL, Chen TH. Polymethylmethacrylate augmentation of pedicle screw for osteoporotic spinal surgery: a novel technique. *Spine* 2008;33(10):E317–24. doi: 10.1097/BRS.0b013e31816f6c73.

23. Choma TJ, Pfeiffer FM, Swope RW, Hirner JP. Pedicle screw design and cement augmentation in osteoporotic vertebrae: effects of fenestrations and cement viscosity on fixation and extraction. *Spine* 2012;37(26):E1628–32. doi: 10.1097/BRS.0b013e3182740e56.

24. Waits C, Burton D, McIff T. Cement augmentation of pedicle screw fixation using novel cannulated cement insertion device. *Spine* 2009;34(14):E478–83. doi: 10.1097/BRS.0b013e3181a8f663.

25. Kayanja M, Evans K, Milks R, Lieberman IH. The mechanics of polymethylmethacrylate augmentation. *Clin Orthop Relat Res* 2006;443:124–30. doi: 10.1097/01.blo.0000200243.60426.57.

26. Blattert TR, Glasmacher S, Riesner HJ, Josten C. Revision characteristics of cement-augmented, cannulated-fenestrated pedicle screws in the osteoporotic vertebral body: a biomechanical in vitro investigation. Technical note. *J Neurosurg Spine* 2009;11(1):23–7. doi: 10.3171/2009.3.SPINE08625.

27. Sarzier JS, Evans AJ, Cahill DW. Increased pedicle screw pullout strength with vertebroplasty augmentation in osteoporotic spines. *J Neurosurg* 2002;96(3):309–12.

28. Konno S, Olmarker K, Byröd G, et al. The European Spine Society AcroMed Prize 1994. Acute thermal nerve root injury. *Eur Spine J* 1994;3(6):299–302.

29. Wilkes RA, Mackinnon JG, Thomas WG. Neurological deterioration after cement injection into a vertebral body. *J Bone Joint Surg Br* 1994;76(1):155.

30. Zindrick MR, Wiltse LL, Widell EH, et al. A biomechanical study of intrapeduncular screw fixation in the lumbosacral spine. *Clin Orthop Relat Res* 1986; 203:99-112.

31. Coe JD, Warden KE, Herzig MA, McAffee PC. Influence of bone mineral density on the fixation of thoracolumbar implants. A comparative study of transpedicular screws, laminar hooks, and spinous process wires. *Spine* 1990;15(9):902–7.

32. Hirano T, Hasegawa K, Takahashi HE, et al. Structural characteristics of the pedicle and its role in screw stability. *Spine* 1997;22(21):2504-10.

33. Okuyama K, Sato K, Abe E, et al. Stability of transpedicle screwing for the osteoporotic spine. An in vitro study of the mechanical stability. *Spine* 1993;18(15):2240-5.

34. Halvorson TL, Kelley LA, Thomas KA, et al. Effects of bone mineral density on pedicle screw fixation. *Spine* 1994;19(21):2415-20.

35. Dawson JM, Boschert P, Macenski MM, Rand N. Clinical relevance of pull-out strength testing of pedicle screws. In: Melkerson MN, Kirkpatrick JS, Griffith S (Eds.) Spinal Implants: Are we evaluating them appropriately? Bridgeport, NJ: ASTM International;2003:68-77. doi: 10.1520/STP11134S.

36. Chapman JR, Harrington RM, Lee KM, et al. Factors affecting the pullout strength of cancellous bone screws. *J Biomech Eng* 1996;118(3):391-8. doi:10.1115/1.2796022.